AN EXPERIMENTAL STuDY TO INVESTIGATE THE UPPER HEATING AND COOLING EFFECT ON NATURAL CONVECTION HEAT TRANSFER THROUGH A HORIZONTAL RECTANGULAR ENCLOSURE

Tamir K. Salim
Tikrit University- College of Engineering
Mechanical department

ABSTRACT

In this study an experimental work has been conducted to investigate the natural convection through a rectangular enclosure fixed horizontally. The upper surface for the apparatus has been heated and cooled. The test apparatus has been manufactured first, and then thermocouples have been fixed in proper positions. Then many readings, for temperatures, have been registered for each thermocouple. These readings have been taken for different mass flow rates of cooling water with different heat fluxes. These experiments have been conducted for the range of Rayleigh number $(4*10^5 \leq Ra \leq 5*10^6)$, and for the range of water mass flow rates in cooling region (0.009 kg/s≤ $\dot{m}$ ≤0.04 kg/s). Four tests for each mass flow rates of water have been conducted, for each one of them five values of heat flux have been used in heating. It has been noticed that the surface temperature of experiments section increased to approach from heating region and the same behavior of temperature inside the section, with appearance stagnation region and not change of air temperature on center region for the apparatus. The study shows that Nusselt number decreases by (50.4 %) in cooling region, and Nusselt number value increases by (33%) in heating region as the mass flow rate of water decreases by (77.5%) for the highest and lowest heat flux. Also, Nusselt number decreases by (57.5%) as the heat flux decreases by (95%) for the highest and lowest water mass flow rate. An experimental correlation has been adopted between average Nusselt number against average Rayleigh number (Ra)

for both heating and cooling region is $1 + 0.016\left(\dfrac{Ra^{0.348}}{0.303} - 1\right)$.

Key words: Natural convection, Rectangular, enclosure, heating and cooling, Horizontal .

دراسة تجريبية لبيان تأثير التسخين والتبريد من الأعلى على انتقال الحرارة بالحمل الحر خلال حيز مغلق أفقي مستطيل الشكل

ثامر خلف سالم
جامعة تكريت-كلية الهندسة
قسم الميكانيك.

الخلاصة

تم في هذه الدراسة أجراء تجارب عملية لقياس الحمل الطبيعي خلال حيز مغلق مستطيل الشكل مثبت بوضع أفقي . السطح العلوي للجهاز تم تبريده وتسخينه. لقد تم تصنيع جهاز الاختبار أولاً ثم تم تثبيت المزدوجات الحرارية عليه بعدها أخذت قراءات متعددة لدرجات الحرارة لكل مزدوج على انفراد. وقد أخذت القراءات المذكورة لتدفقات كتلية مختلفة لماء التبريد مع تغير الحمل الحراري.

أجريت هذه التجارب للمدى من عدد رايلي ($4*10^5 \leq Ra \leq 5*10^6$)، ولمدى من معدل التدفق الكتلي للماء في منطقة التبريد ($0.009 \leq \dot{m}_w \leq 0.04 kg/s$). أجريت أربعة اختبارات للتدفق الكتلي للماء يقابل كل منها خمس قيم للفيض الحراري في منطقة التسخين. لوحظ أن درجة الحرارة لسطح مقطع الاختبار تزداد بالاقتراب من منطقة التسخين وبنفس التصرف لدرجات الحرارة داخل المقطع مع ظهور منطقة ركود وعدم تغير في درجات الحرارة بشكل ملحوظ في المنطقة الوسطية للجهاز. تبين من هذه الدراسة أن عدد نسلت يقل بنسبة (٥٠.٤%) في منطقة التبريد و يزداد عدد نسلت بنسبة (٣٣%) في منطقة التسخين مع نقصان معدل التدفق الكتلي للماء بنسبة (٧٧.٥%) عند أعلى واقل فيض حراري. أيضا، ان عدد نسلت يقل بنسبة (٥٧.٥ %) بنقصان الفيض الحراري بنسبة (٩٥ %) عند أعلى واقل تدفق كتلي للماء. استنبطت من هذه الدراسة علاقة تجريبية بين معدل عدد نسلت (**Nu**) يقابل معدل عدد رايلي لكلا منطقتي التبريد والتسخين وهي،

$$1 + 0.016\left(\frac{Ra^{0.348}}{0.303} - 1\right).$$

الكلمات الدالة: حمل طبيعي ، مستطيل، حيز مغلق ، تبريد و تسخين، أفقي.

Nomenclature

Symbol	Description	Unit
A_s	Surface area	m^2
B	Enclosure width	m
Cp	Specific heat	J.kg-1. K-1
EIP	Electrical input power	Watt
g	Acceleration due to gravity	m/s^2
h	Heat transfer coefficient	$W.m^{-2}.^oC^{-1}$
I	Electrical current	Ampere (A)
k	Thermal conductivity	$W.m^{-1}.^oC^{-1}$
L	Enclosure length	m
$\dot{m}_w$	Mass flow rate of water	$kg.s^{-1}$
Nu	Nusselt number	---
Ra	Rayleigh number	---
Pr	Prantel number	---
Q_g	Heat generated	$W. m^{-2}$
q_c	Convection heat flux	$W. m^{-2}$
q_r	Radiation heat flux	$W. m^{-2}$
Q_w	Cooling heat	Watt
T	Temperature	^oC
V	Heater voltage	Volt (V)
x	Axial distance	m

Greek symbols

ε	Emissivity	--
δ	Enclosure thickness	m

ρ	Density	$kg.m^{-3}$
α	Thermal diffusivity	$m^2\,s^{-1}$
ν	Kinematic viscosity	$m^2.s^{-1}$
μ	Dynamic viscosity	$kg.m^{-1}.s^{-1}$
β	Volume expansion coefficient	K^{-1}
σ	Stefan-Boltzmann constant	$= 5.67 \times 10^{-8}\ W\ m^{-2}\ K^{-4}$

Subscripts

C	Cold	--
fL	Film	--
f	Fluid (air)	--
H	Hot	--
i	Inlet or (inside)	--
o	outlet	--
s	surface	--
w	water	--

INTRODUCTION

Steady state natural convection from rectangular enclosures and square ducts has many engineering applications in cooling of electronic components, design of solar collectors and heat exchangers. Survey of the literature shows that correlations for natural convection from vertical and horizontal plates, vertical and horizontal cylinders, spheres, vertical channels and elliptic cylinders are reported for different thermal boundary conditions. However, limited numbers of experimental studies were concerned with heat transfer through rectangular enclosures and square ducts heated and cooled from above**(Zeitoun and Mohamed, 2005)**.

(Al-Bahi et al., 2002); had studied numerically laminar natural convection heat transfer in an air filled vertical square cavity differentially heated with a single isoflux discrete heater (heater length/enclosure height= 0.125) on one wall and the opposite wall represented a heat sink with top and bottom adiabatic surfaces. The time dependent two-dimensional conservation equations of mass, momentum, and energy are solved employing a forward time central space implicit finite difference scheme. The streamlines and isotherms for different heater locations (the distance from the heater center to the bottom of the cavity/ enclosure height= 0.25-0.75) and Rayleigh numbers (10^3–10^6) were obtained. Their results showed that for small heaters the flow was characterized by a single circulation cell, which prolonged to an elliptical shape at high Rayleigh numbers (10^6) with distortion towards the location of the heater. At low Rayleigh numbers (10^3–10^4), heat transfer by conduction was dominating and Nusselt number was nearly constant. The conducted that the local Nusselt number decreased along the heater length from the leading edge with slight enhancement at the trailing edge.

Effects of thermo-acoustic wave motion on the developing natural convection process in a compressible gas-filled (Nitrogen and Helium) square enclosure were investigated numerically by **(Murat and Bakhtier, 2003);** the left wall temperature was raised rapidly (impulsively or gradually) while the right wall was held at a specified temperature. The top and the bottom walls of the enclosure were considered thermally insulated. The numerical solutions of the full Navier–Stokes equations were obtained by employing a highly accurate flux-corrected transport algorithm for the convection terms and by a central differencing scheme for the viscous and diffusive terms. Thermo acoustic waves were generated by increasing the left wall temperature of the enclosure impulsively (suddenly) or gradually and rapidity of the wall heating process was observed to be the leading parameter on the strength of the thermo acoustic waves.

(**Rahman and Sharif, 2003**); investigated numerically free convective laminar flow of a fluid with or without internal heat generation in rectangular enclosures of different aspect ratios and at various angles of inclination. Two principal parameters for this problem were the external Rayleigh number which represented the effect due to the differential heating of the side walls, and the internal Rayleigh number which represented the strength of the internal heat generation. Results were obtained for a fixed external Rayleigh number (2×10^5), with internal Rayleigh number (0) (without internal heat generation), and also with internal Rayleigh number (2×10^5) (with internal heat generation).Flow patterns and isotherms did not show any significant difference between the cases with and without internal heat generation other than slight shift and changes in stream function and isotherm values as long as the internal Rayleigh number was less than or equal to the external Rayleigh number. Local heat flux ratios along the hot and the cold walls decreased monotonically in the flow direction for a major downstream portion. At certain inclinations the local heat flux ratios increased initially and then decreased.

The Steady laminar natural convection in air-filled, 2-D rectangular enclosures heated from below and cooled from above, was studied numerically for a wide variety of thermal boundary conditions at the sidewalls by (**Massimo C., 2003**). He used mass, momentum and energy transfer governing equations which was solved by developed numerical model based on the SIMPLER algorithm. The study was carried out for the range of aspect ratio $(0.66 \le A \le 8)$, and the range of Rayleigh number $(10^3 \le Ra \le 10^6)$. He found that the heat transfer effectiveness of the bottom wall increased as each adiabatic sidewall, and the heat transfer rate from any heated or cooled boundary surface of the enclosure increases as the Rayleigh number increased. While the local heat fluxes from the top and bottom walls are strictly dependent on the thermal boundary conditions. the heat transfer rate from the heated or cooled sidewalls was independent of the thermal configuration of the enclosure.

(**Zeitoun and Mohamed,2006**); had reported numerical simulations of natural convection heat transfer from isothermal horizontal rectangular cross section ducts in air. Their results showed as the aspect ratio increases, separation and circulation occurs on the top surface of the cross section duct at fixed Rayleigh number and the corresponding behavior had been observed through the isotherms. They had also obtained a general correlation using the aspect ratio (Γ) as a parameter:-

$$\mathbf{Nu = \left[0.9\Gamma^{-0.061} + 0.371\Gamma^{-0.114}Ra^{0.1445}\right]^2} \quad 700 \le Ra \le 10^8$$

The study of laminar and transition to turbulence natural convection heat transfer from the outer surface of rectangular ducts in air with their axis horizontally, was investigated experimental by (**Mohamed,2007**); Five ducts had been used with aspect ratios of 2,1 and 0.5. The ducts heated using internal constant heat flux heating elements. Two distinct flow regimes were observed; namely laminar and transition to turbulence. Their results showed at low values of convection heat flux and characterized due to decrease in value of Nusselt numbers at any fixed longitudinal x station on the duct's surface, and Nusselt number increased as x increased along the duct's surface for any value of the heat flux. They had also obtained a general correlation of average Nusselt numbers by using a parameters, aspect ratio (Γ), area ratio (κ) and (Ra):-

$$\mathbf{Nu = 0.256(Ra)^{0.179}\kappa^{0.367}\Gamma^{-0.385}} \quad \kappa\langle100,,3*10^7 \le Ra \le 6*10^8$$

Numerical simulation of turbulent natural convection in a square enclosure with localized heating from below and symmetrical cooling from the vertical side walls were reported by (**Sharma A. etal. ,2007**), The heat source was considered to be centrally located at the bottom wall with different heated widths, which was assumed to be either isothermal or with isoflux. Distributions of streamlines and temperature fields were obtained. The dependence of the Nusselt number on the heated width was found to be completely different rot the isothermal and isoflux heating cases.

(**Hakan f. & Eiyad A., 2008**), studied Numerical of natural convection in partially heated rectangular enclosures filled with nanofluids. They used finite volume to solve the governing equation.

The Calculations were performed for Rayleigh number $(10^3 \leq Ra \leq 5*10^5)$, height of heater $(0.1 \leq h \leq 0.75)$, location of heater $(0.25 \leq y_p \leq 0.75)$, aspect ratio $(0.5 \leq A \leq 2)$ and volume fraction of nanoparticles $(0 \leq \phi \leq 0.2)$. They found the heat transfer increased with increases of height of the heater. Also, the heater location affected the flow and temperature fields when using nanofluids. The nanofluids increased with increasing the value of volume fraction of nanoparticles. the enhancement of heat transfer in rectangular enclosures, dependent on the presence of nanoparticles.

Mathamitical simulation of the transient turbulent natural convection in the rectangular enclosure having finite thickness walls, were studied by **(Geniy V. etal.,2010)**, they used the Navier-stokes equation to solve the turbulence model with wall function. The study was carried out for Grashof number $(10^8 \leq Gr \leq 10^{10})$, the transient factor $(0\langle\tau\langle 1000)$ and thermal conductivity ratio ($K_{1,2}$=5.7*10^{-4}, 6.8*10^{-5}). They found that increasing Gr is reflected in reduction of a thermal boundary layer thickness, and the increased in transient factor leads to increment in average Nusselt number. The decrease in thermal conductivity ratio leads to the diminution of the generalized heat transfer coefficient and increased in average Nusselt number. A correlation was obtained between Grashof number and average Nusselt number is:- $\mathbf{NU_{avg} = 0.53 * Gr^{0.19}}$

EXPERIMENTAL WORK

Natural convection heat transfer is one of the most important convection transfers so we conduct an experiment natural convection in a rectangular enclosure. A **photo (A-1)** shows the test section , and **fig.(B-1)** illustrates the schematic drawing of the test section.

A rectangular enclosure made of galvanized iron oriented horizontally is used. The cross section area of enclosure is square, its thickness (δ) and width **enclosure (B)** are (10cm), and the length was (100 cm). The dimensions of cooling tank are $(10\times10\times50cm)$. The active heated length is only (50 cm) and cooling length is only (50 cm).

The rectangular surface temperature was measured by (50) thermocouples (T type) which are positioned on all apparatus surface, four thermocouples are positioned for five locations, (2) thermocouples to measure the temperature at the ends the apparatus section and (5) thermocouples in five locations to measure the inside air temperature in the center of the apparatus section, also (2) thermocouples has been used to measure the temperature of the inlet and outlet water from cooling tank. Another thermocouple is used to measure the laboratory ambient temperature.

The upper surface test section was heated electrically using coil and an electrical resistance on the upper wall of (5m) in length with a resistance $(1\Omega/m)$. To reduce the heat losses the test section is thermally insulated with fiber glass of (10cm) in thickness. The two ends of the apparatus section and other surfaces were insulated electrically and thermally using fiber glass only.

The heater was supplied with an alternative electrical power using converter that supplies with a steady voltage through a voltage regulator (220 V). An Ameter was used to measure the current pass through the heater with accuracy (10^{-4} A).

The cooling water flow rate can be controlled by two valves for inlet and outlet water from the cooling tank, the mass flow rate of water is calculated by using a (1000 ml) glass container and stop watch.

CALCULATION PROCEDURES

Before the experiments test starts, the thermocouples are calibrated using distilled water and crushed ice bath in the range of (0-100)^{o}C. Mercury bulb thermometer was immersed together with a thermocouple and water temperature was recorded. Sample calibration curve is shown in **fig.(2)**. The laboratory ambient temperature is within the range (15-20 ^{o}C). The test procedure can be listed as follow:-

1-   Control the water mass flow rate by inlet valve.
2-   The test section is set to the proper voltage and this is achieved using a variable transformer.
3-   After (1.5-2 hr) the system reaches the steady state condition. The enclosure surfaces temperatures, the inlet and outlet water temperatures, the water mass flow rate through the cooling tank, the laboratory temperature and the heater voltage and current have been registered.

The heat generated (q_g) is dissipating from the enclosure surface by convection and radiation.

$$\mathbf{EIP = I * V} \tag{1}$$

$$\mathbf{Q_g = \dfrac{EIP}{A_s}} \tag{2}$$

Where $\mathbf{A_s = 0.5B * L}$

$$\mathbf{Q_g = q_c + q_r} \tag{3}$$

Where q_c and q_r, are the fraction of the heat flux dissipating from the enclosure surface by convection and radiation, respectively which can be calculated as (**Mohamed, 2007**):

$$\mathbf{q_r = \varepsilon\sigma\left(T_H{}^4 - T_C^4\right)} \tag{4}$$

Where (T_H and T_C) is represented in **Figre1**:
$T_{H=}\, T_{H1}$: is the upper surface temperature in heating region for right side.
$T_{C=}\, T_{C1}$: is the lower surface temperature in heating region for right side.
$T_{H=}\, T_{H2}$: is the lower surface temperature in cooling region for left side.
$T_{C=}\, T_{C2}$: is the upper surface temperature in cooling region for left side.
ε is the surface emissivity of the enclosure and it is estimated as 0.3 for galvanized iron (**Siegel, 1992).**

The film temperature for the air is calculated using the following equation (**Holman, 1977**):

$$\mathbf{T_{fL} = \dfrac{T_H + T_C}{2}} \tag{5}$$

The characteristic of the air are calculated through the test section which are varied depending on in the film temperature of the air and these are calculated using the following empirical equation (**John, 2003**):

$$\mathbf{\rho_f = 1.21003 + 7.4715 * 10^{-3}\,T_{fL} - 3.8919 * 10^{-5} * T_{fL}^2 + 4.54786 * 10^{-8}\,T_{fL}^3} \tag{6}$$

$$\mathbf{\mu_f = 1.577 * 10^{-4} - 1.285 * 10^{-6}\,T_{fL} + 3.836 * 10^{-9}\,T_{fL}^2 - 3.662 * 10^{-12}\,T_{fL}^3} \tag{7}$$

$$\mathbf{k_f = 0.155 - 1.236 * 10^{-3}\,T_{fL} + 3.760 * 10^{-6}\,T_{fL}^2 - 3.588 * 10^{-9}\,T_{fL}^3} \tag{8}$$

$$\mathbf{Pr_f = 2.692 - 1.691 * 10^{-2}\,T_{fL} - 4.799 * 10^{-6}\,T_{fL}^2 - 3.588 * 10^{-9}\,T_{fL}^3} \tag{9}$$

$$C_{pf} = 825.885 + 1.627 T_{fL} - 4.97 * 10^{-3} T_{fL}^2 + 5.205 * 10^{-6} T_{fL}^3 \qquad (10)$$

$$\alpha_f = -0.2315 + 2.362 * 10^{-3} T_{fL} + 2.143 * 10^{-5} T_{fL}^2 - 6.99 * 10^{-9} T_{fL}^3 \qquad (11)$$

Where the quantity of the heat transfer (Q_w) from the air in cooling region is calculated as follow (**Holman, 1977**):

$$Q_w = \dot{m}_w C_{pw} (T_{wo} - T_{wi}) \qquad (12)$$

Local convection heat transfer coefficient and local Nusselt number have been calculated indirectly measured respectively using the following equations (**Mohamed, 2007**):

$$h_x = \frac{q_c}{\left(T_{H_x} - T_{C_x}\right)} \qquad (13)$$

$$Nu_x = \frac{h_x . \delta}{k} \qquad (14)$$

Then the overall longitudinal average $\overline{h}$ can calculated as flow (**Mohamed, 2007**):

$$\overline{h} = \sum_{x=1}^{5} h_x / 5 \qquad (15)$$

The non-dimensional overall average Nusselt and Rayleigh numbers are calculated as follow (**Mohamed, 2007**):

$$Nu = \frac{\overline{h} . \delta}{k} \qquad (16)$$

$$Ra = \frac{g \beta \left(T_{H_x} - T_{C_x}\right) . \delta^3}{\nu \alpha} \qquad (17)$$

Where $\quad \nu = \dfrac{\mu_f}{\rho_f} \quad$ and $\quad \beta = \dfrac{1}{T_{fL}}$

Four tests have been carried out (0.04, 0.02, 0.14 and 0.009 kg/s). Water is used to cool the half upper surface. And for each mass flow rate the heat generated is changed (147, 490, 1054, 1708 and 2940 W/m^2). The previous test have been repeated ones for each change in water mass flow rate.

RESULTS AND DISCUSSIONS

Twenty tests had been carried out for each of the following variables.
1. the mass flow rate of water have been varied within the range (0.009-0.04 kg/s) and this was done four times.
2. the heat flux have been varied within the range (147-2940 W/m^2) and this was done five times.

The effect of mass flow rate on the temperature ratio (the ratio between the top surface temperatures and the temperature of the air in the center of the enclosure) at constant heat flux is shown in **Figures 3-7.** In the cold region this ratio is almost constant no mater what is the mass flow rate at any heat flux. This is happening because the cold air is moving downward and the air in the center of the enclosure is almost has the temperature of the top cold surface, then the temperature ratio rises up as moving toward the hot region because the air can't neither moves downward because it's density is getting lower nor cross the top solid surface, so it moves sideward preferring the cold half side. For these reasons the temperature ratio is increasing and gets it's highest value at (x/L=0.67), this region can be considered a stagnation region. The decreasing in the section apparatus temperature ratio at the end is justified by the heat loss at that region. At a specific heat flux when the mass flow rate increases more heat is convected which decreases the temperature ratio.

Figures 8-11 show the effect of changing heat flux at constant mass flow rate on the temperature ratio. The same previous general behavior is observed. At a specific mass flow rate as the heat flux increases the top surface temperature in the hot region is getting higher than the temperature of the air in the center of the enclosure which means higher temperature ratio particularly at (x/L=0.67) , then because of the thermal losses from the end the temperature ratio decreases.

Figures 12-16 illustrates the effect of mass flow rate on local Nusselt number (Nu_x) along the enclosure at constant heat flux for each figure. Nu_x distribution suffers from fluctuating along the enclosure. The highest Nu_x value is related to the convection created by the top cooling at ($x/L = 0.33$), while the lowest can be observed at ($x/L = 0.67$) where the top surface is heated. This means that the lowest heat transfer occurred in this part of the enclosure. Referring to the value of Nu_x (nearly equal 1) this region can be considered as a stagnation region, that's happened because the heat transferred by strong bouncy- induced flows can not be transferred upward so that the heat is rather transferred sideward practically toward the cold region causing high heat convection in this region. All heat fluxes Nu_x distribution has the same behavior. The Increasing heat flux will increase the heat convected in the enclosure leading to increase Nu_x. When the mass flow rate decreases at (0.014 and 0.009 kg/s) less heat will be convected at low heat flux (147 and 490 W/m^2) and causing convergence Nu_x values in the cold half of the enclosure, as shown in **Figures 12 and 13.**

The same general behavior for Nu_x distribution is observed when the heat flux change at fixed water mass flow rate as shown in **Figures 17-20**. As the mass flow rate increases more heat is convected from the hot surface to the cold surface which will cause higher Nu_x for any heat flux, so that at ($\dot{m} = 0.04$ kg/s) witness the highest Nu_x at ($x/L = 0.33$), this is because of increasing the heat convected between the coming hot air from the hot region and the cold surface. At ($x/L = 0.67$) Nu_x does not affected by changing mass flow rate and it's still presents a stagnation region. Also ,it can be seen at higher heat flux (Qg=2940 W/m^2) When the mass flow rate decreases at (0.014 and 0.009 kg/s) more heat will be convected at ($x/L = 0.33$) causing higher Nu_x value and causing convergence in Nu_x values in the cold half of the enclosure, as shown in **Figures 19 and 20.**

The increase of average Rayleigh number causes considerable increasing in the average value of Nusselt number for different value of heat fluxes. And this was shown in **Figure 21**, this is because of the effect of increasing convected heat as the heat generated increases. The average value of Nusselt number is decreasing by (57.5%) as the heat generated decreases by (95%).

Figure 22 shows the relation ship between the average Nusselt number and the average Rayleigh number for different values of water mass flow rates. It could be seen that the average value of Nusselt number is increasing with the increase of average Rayleigh number and this is for all different water mass flow rates, this is because increasing heat transfer coefficient. The average value of Nusselt number decreases by (50.4%) as the water mass flow rate decreases by (77.5%), this is because the water gets hotter and the heat transfer reduced and Nu will be reduced subsequently.

The case when there is no mass flow rate is chosen to predict the results of present work, as declared in **Figure 23.** In this case since the enclosure is heated from above and there is no fluid flow (Nu equals 1) **(Bejan and Kraus, 2003)**. The maximum difference between the present work and the case above is (19%) which can be accepted.

Figure 24 compares the regression of the lines and experimental data. The following correlation is obtained for the present data is:

$$Nu = 1 + 0.016\left(\frac{Ra^{0.348}}{0.303} - 1\right) \tag{18}$$

For $(4*10^5 \leq Ra \leq 5*10^6)$, With an error band of $(\pm 15\%)$.

The comparison between the correlation obtained from equation (18) with reference **(Bejan and Kraus, 2003)** is shown in **Figure 25**, it can be seen the error percentage don't exceed (19 %), which can be accepted.

CONCLUSIONS

From this study the following conclusion be deduced:-.

1. The internal temperature increases with increasing the heat flux and decreases with increasing the water mass flow rate. This is because of the Phenomenon of separating the cold air to be settled in the bottom and the hot air to be settled in the supreme.

2. A stagnation region is observed below the top heated surface. This happens because the heated fluid always rises up, but since the hot surface is in the top the air can't move upward and instead it moves sideward. In this case the hot air prefers to move toward the cold region causing the highest heat transferred in the enclosure.

3 The stagnation region and the highest heat transfer region can be observed in the same location in the enclosure at any mass flow rate and any heat transfer flux.

4. Increasing the mass flow rate and the heat flux causes increasing the bouncy- induced flow strength which benefits the heat transfer.

5. When ($\dot{m}_w = 0$ kg/s) the present data has a good agreement with the case of horizontal rectangular enclosure heated from above with no fluid flow.

6. The values of locally Nusselt number have its highest values for highest value of water mass flow rate with increases the value of Rayleigh number.

7. An empirical relation between the average values of Nusselt number with average value of Rayleigh number for all cases **(equation (18))**.

REFERENCES

AL-Bahi, A.M., Radhwan, A.M. and Zaki, G.M.,"Laminar natural convection from an isoflux discrete heater in a vertical cavity,, The Arabian for science and Engineering, Vol.27, No.2C, December (2002).

Bejan, A. and Kraus, A. D., "Heat Transfer Handbook," John Wiley & Sons, 2003.

Geniy V. K., Mikhail A. S. ," Numerical simulation of turbulent natural convection in a rectangular enclosure having finite thickness walls", International Journal of Heat and Mass Transfer, vol. 53, pp.163-177, (2010).

Hakan F. O. and Eiyad A. N.," Numerical study of natural convection in partially heated rectangular enclosures filled with nanofluids", international journal of Heat and Fluid flow , vol. 29, pp.1326-1336, (2008).

Holman, J. P," Experimental Method for Engineers", McGraw- Hill Book company, 5th Edition,(1977).

John H. Lienhord IV and John H. Lienhord V, " A Heat Transfer Text Book", 3rd edition, pp. 714, (2003), http://web.mit.edu/ Lienhord.

Massimo Corcione ," Effects of the thermal boundary conditions at the sidewalls upon natural convection in rectangular enclosures heated from below and cooled from above", international journal of thermal sciences, vol. 42, pp.199-208, (2003).

Mohamed E. A.," Experimental study of steady state natural convection heat transfer from noncircular metallic ducts", king Saud university college of engineering research center, No. 33/426, January, (2007) .

Murat K. A. and Bakhtier F.I.," Numerical simulation of developing natural convection in an enclosure due to rapid heating",   International Journal of Heat and Mass Transfer, Vol. 46, pp.2253-2261, (2003).

Rahman, M. and Sharif, M.R.," Numerical study of laminar natural convection in incline rectangular enclosures of various aspect ratios," Numerical Heat Transfer, part A, Vol. 44, pp. 355-373, January (2003).

Sharma A.K. , Velusamy K., Balaji C., "Turbulent natural convection in an enclosure with localized heating from below", international journal of thermal sciences, vol. 46, pp.1232-1241, (2007).

Siegel, R. and Howell, J. R.,"Thermal Radiation Heat Transfer," McGraw-Hill,New York, 3rd edition ,(1992).

Zeitoun, O. and Mohamed A.,"Natural convection heat transfer from isothermal horizontal rectangular ducts,"Alexandria Engineering journal, Vol.44, No.5, pp.695-704, September (2005).

Zeitoun, O. and Mohamed A, "Numerical Investigation of Natural Convection Around Isothermal Horizontal Rectangular Ducts," Numerical Heat Transfel, Part A, Vol.50, pp.189-204, (2006).
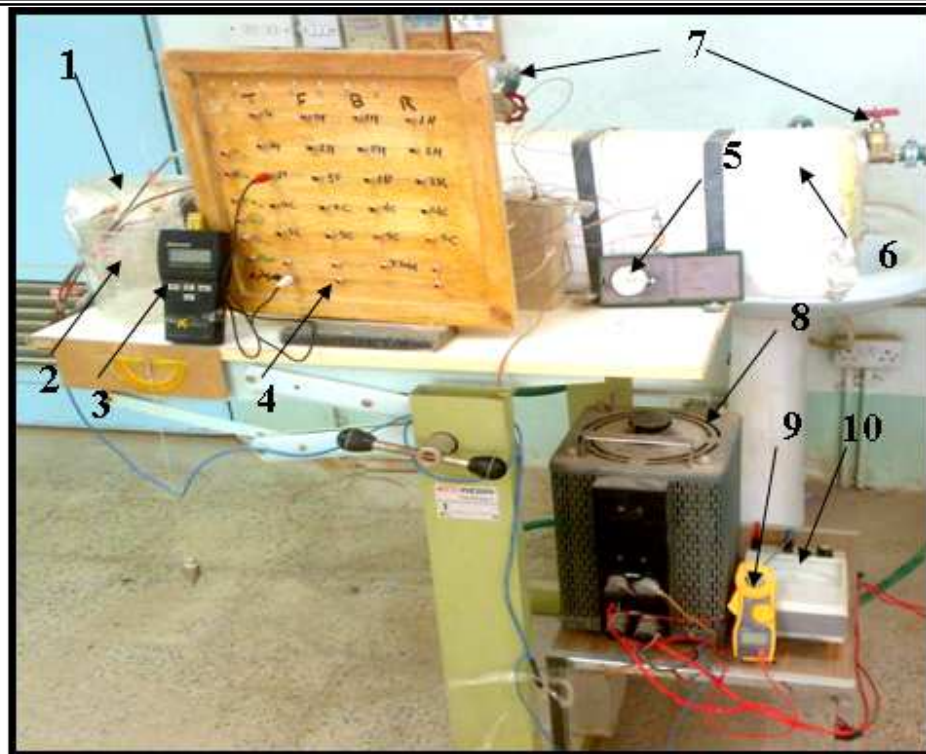
Figure 1-A A photo graph showing the test a parties.
1- Test section, 2- glass container. 3- Thermometer. 4- Meter panel. 5- Stop watch.
6- Cooling tank. 7- Valves. 8- Voltage regular, 9- voltmeter, 10- Ameter
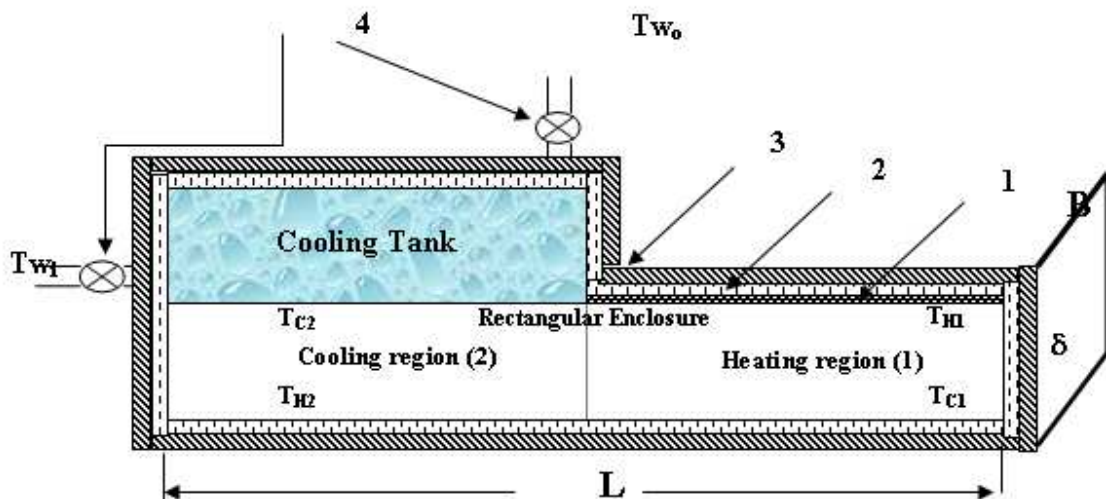
Figure 1-B schematic drawing of the Test section
. 1-thermal resistance, 2- thermal insulator, 3- fibber glass, 4- water valves
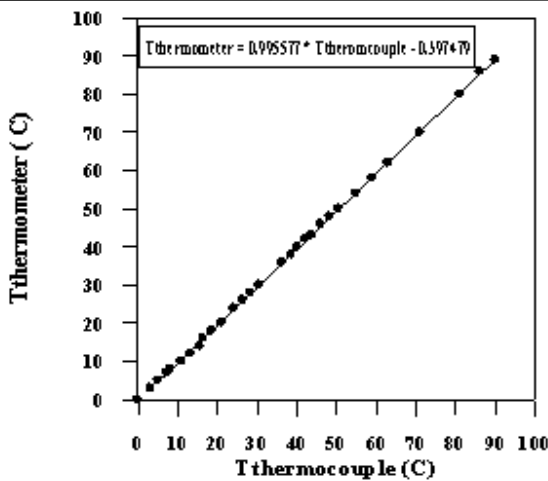
Figure 2 (T) Type thermocouple calibration curve.
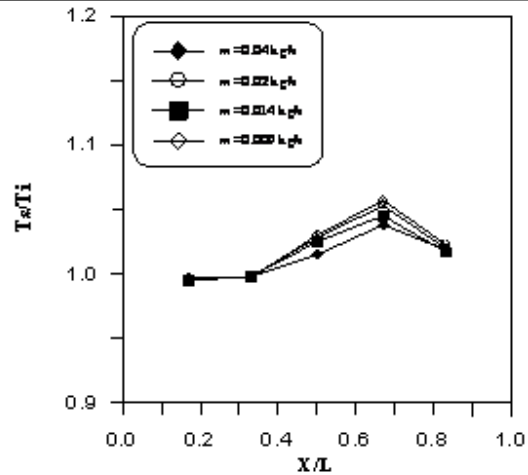
Figure 3 Effect of mass flow rate on the temp. ratio distribution along the enclosure at (Q_g=147W/m^2).
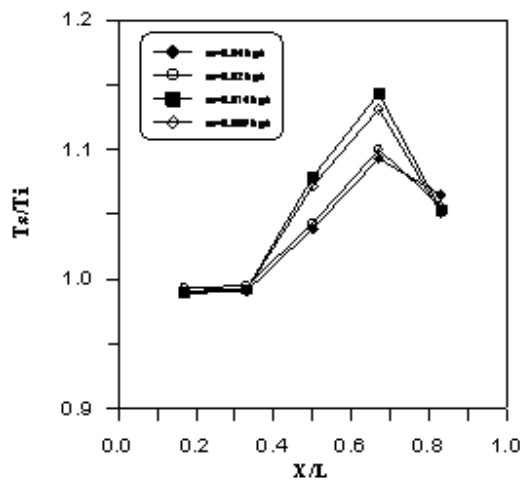
Figure 4 Effect of mass flow rate on the temp. ratio distribution along the enclosure at (Q_g=490 W/m^2).
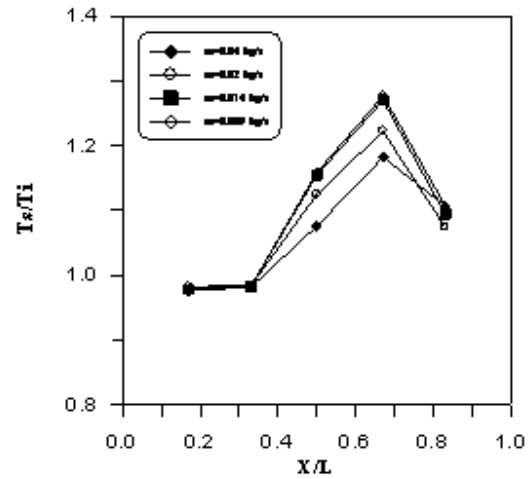
Figure 5 Effect of mass flow rate on the temp. ratio distribution along the enclosure at (Q_g=1054 W/m^2).
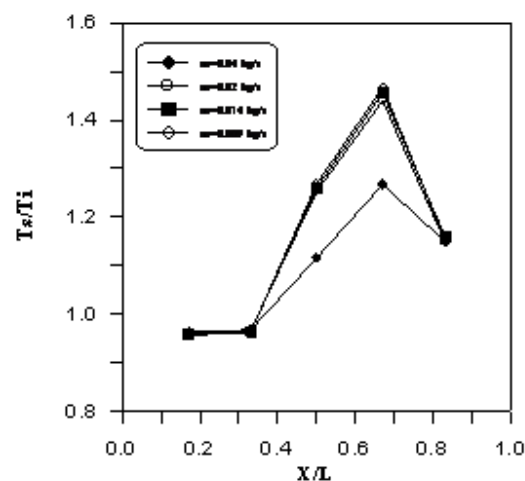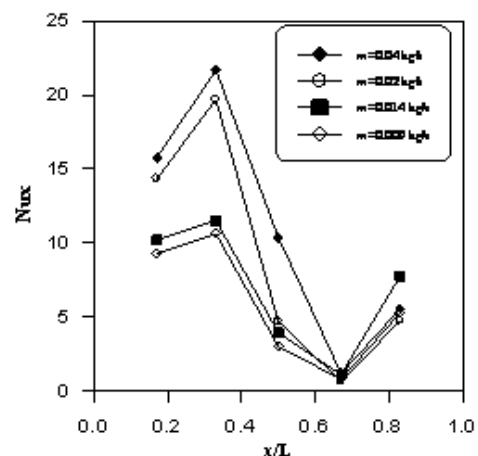

Figure 6 Effect of mass flow rate on the temp. ratio distribution along the enclosure at (Q_g=1708 W/m^2).
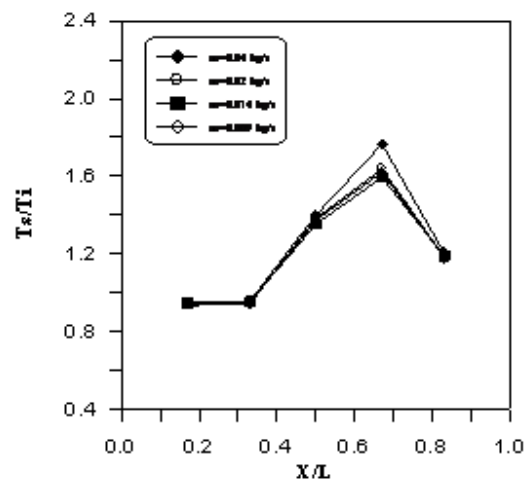
Figure 7 Effect of mass flow rate on the temp. ratio distribution along the enclosure at (Q_g=2940 W/m^2).

55
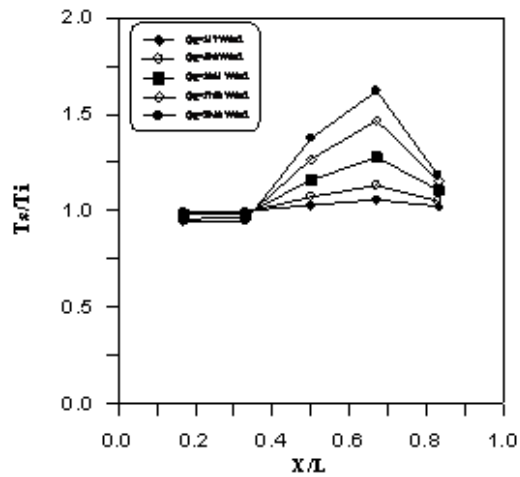
Figure 8 Effect of heat flux on the temp. ratio
=0.009 kg/s). ṁ distribution along the enclosure at (
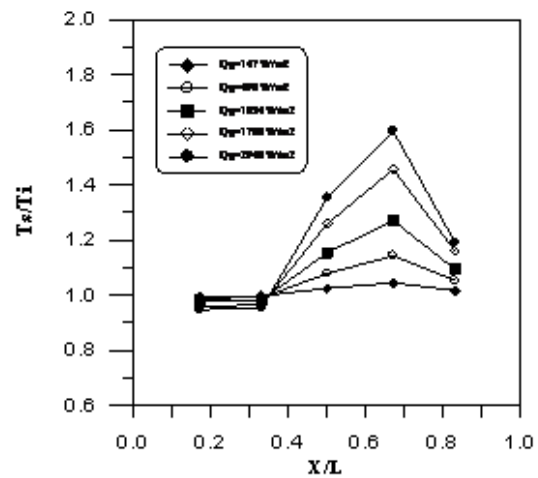
Figure 9 Effect of heat flux on the temp. ratio
=0.014 kg/s). ṁ distribution along the enclosure at (
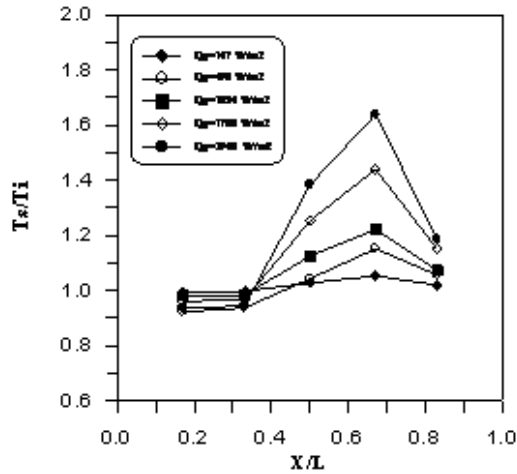
Figure 10 Effect of heat flux on the temp. ratio
=0.02 kg/s). ṁ distribution along the enclosure at (
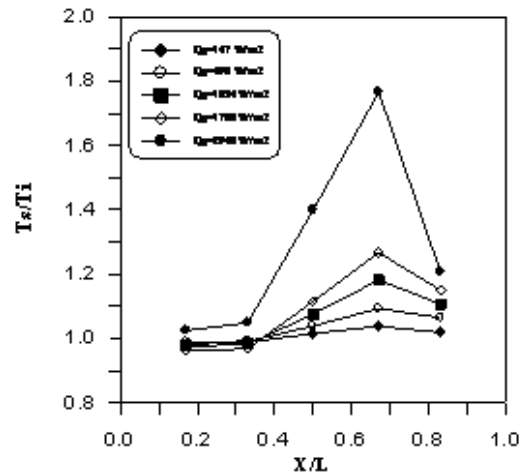
Figure 11 Effect of heat flux on the temp. ratio
=0.04kg/s). ṁ distribution along the enclosure at (
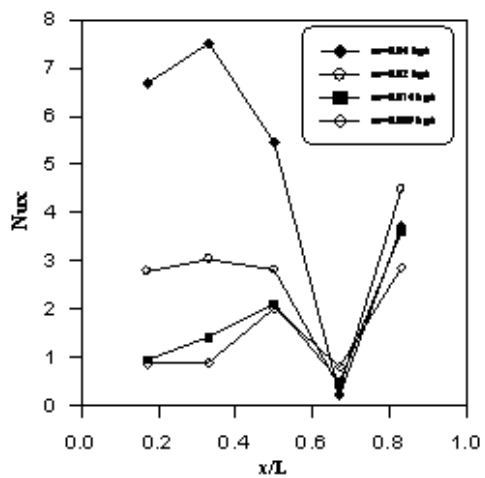
Figure 12 Effect of mass flow rate on local Nusselt
distribution along the enclosure at (Q_g=147 W/m^2).
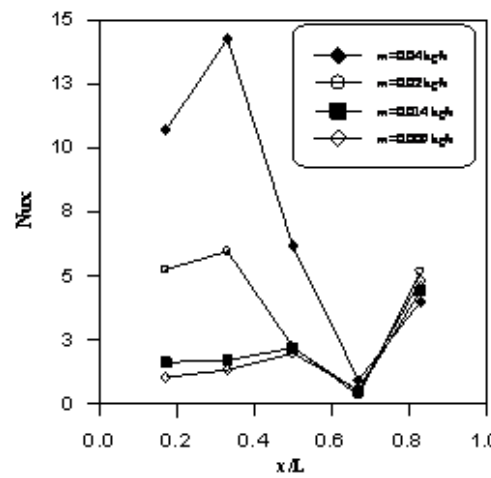
Figure 13 Effect of mass flow rate on local Nusselt
distribution along the enclosure at (Q_g=490 W/m^2).
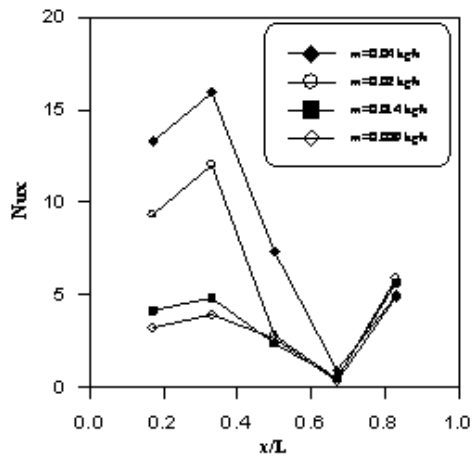
Figure 14 Effect of mass flow rate on local Nusselt distribution along the enclosure at (Q_g=1054 W/m^2).

Figure 15 Effect of mass flow rate on local Nusselt distribution along the enclosure at (Q_g=1708 W/m^2).
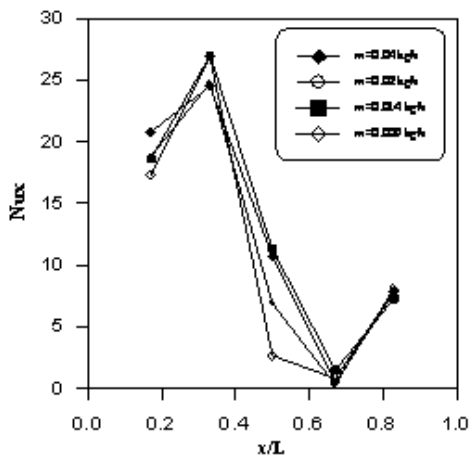
Figure 16 Effect of mass flow rate on local Nusselt distribution along the enclosure at (Q_g=2940 W/m^2).
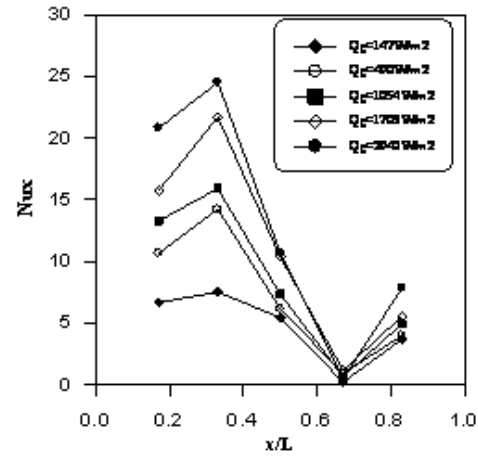
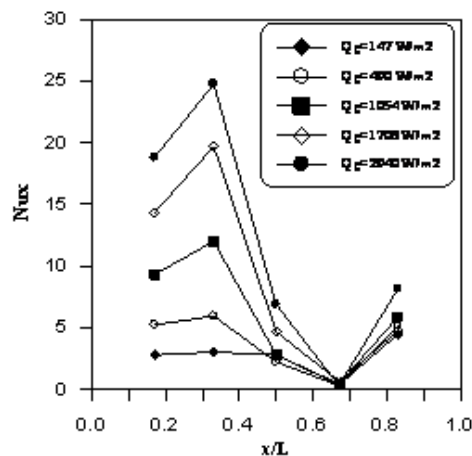**Figure 17** Effect of heat flux on local Nusselt distribution along the enclosure at ($\dot{m}$ =0.04 kg/s).

Figure 18 Effect of heat flux on local Nusselt distribution along the enclosure at ($\dot{m}$ =0.02 kg/s).
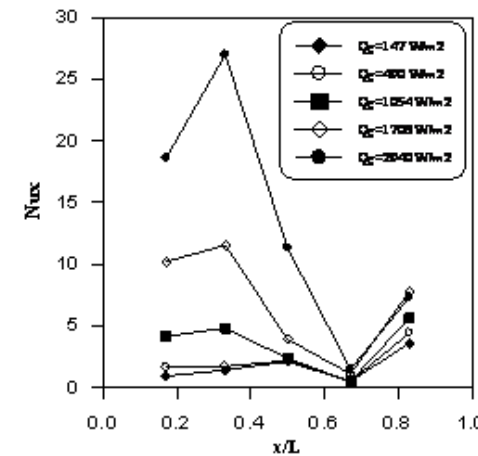
Figure 19 Effect of heat flux on local Nusselt distribution along the enclosure at ($\dot{m}$ =0.014 kg/s).
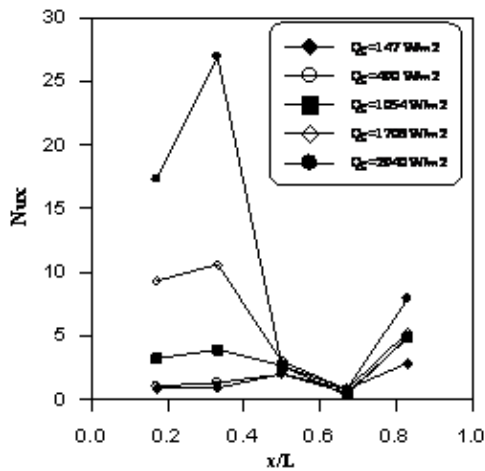
Figure 20 Effect of heat flux on local Nusselt distribution along the enclosure at ($\dot{m}$ =0.009 kg/s).
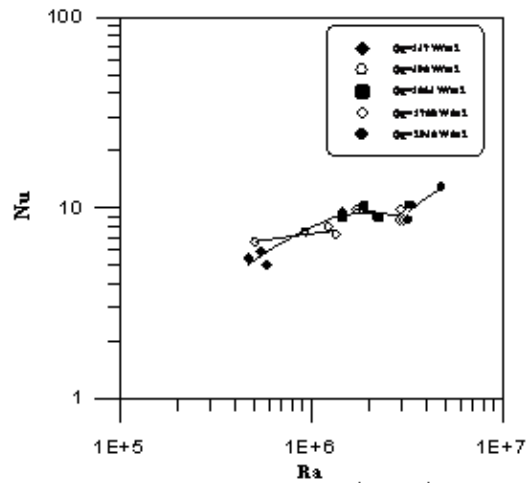

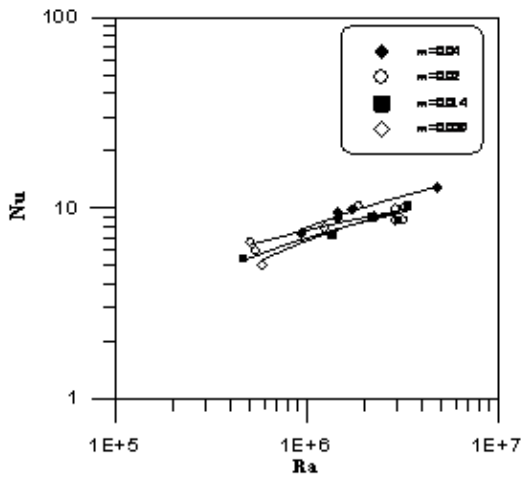**Figure 21** Average Nusselt number versus Raleigh numbers at different heat fluxes.

Figure 22 Average Nusselt number versus Raleigh numbers at different mass flow rates.
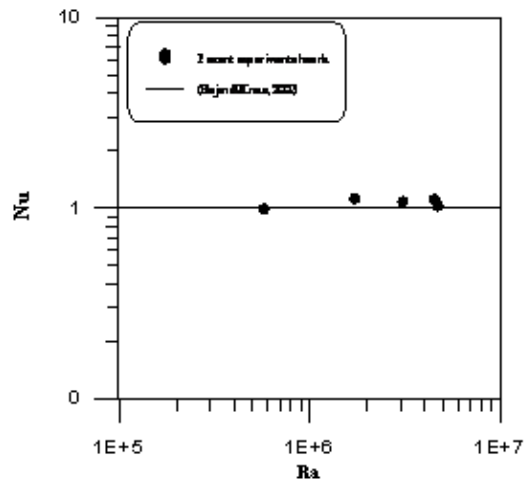

Figure 23 comprision between precent experimental work with **(Bejan&Kraus, 2003)** at ($\dot{m}$ =0.0 kg/s).
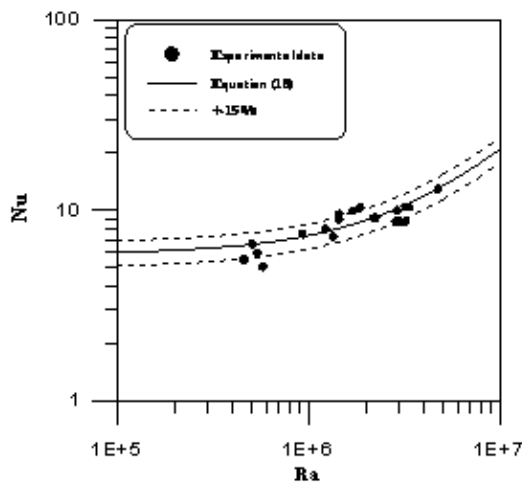

Figure 24 comprision between precent experimental data with the correlation obtained (18).
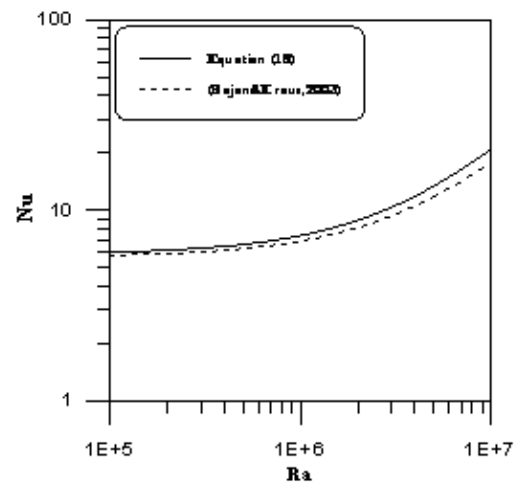

Figure 25 comprision between the correlation obtained (18) with **(Bejan&Kraus, 2003)**.